Chemosphere 301 (2022) 134702

Contents lists available at ScienceDirect

Chemosphere

journal homepage: www.elsevier.com/locate/chemosphere

An improved surface enhanced Raman spectroscopic method using a paper-based grape skin-gold nanoparticles/graphene oxide substrate for detection of rhodamine 6G in water and food

Kandi Sridhar [a,1], Baskaran Stephen Inbaraj [a,1], Bing-Huei Chen [a,b,*]

[a] Department of Food Science, Fu Jen Catholic University, New Taipei City 24205, Taiwan
[b] Department of Nutrition, China Medical University, Taichung 40402, Taiwan

HIGHLIGHTS

- Grape skin-AuNPs/GO based paper SERS method was developed for rhodamine 6G detection.
- Synthesized nanostructures were characterized by UV–Visible, Raman, zeta potential and TEM.
- High enhancement factor was shown for GE-AuNPs (10^4) and GE-AuNPs/GO (10^9).
- Low detection limit and high repeatability/reproducibility were obtained for GE-AuNPs/GO.
- High recovery from tap water, chilli powder, glutinous rice ball and tomato ketchup was shown.

GRAPHICAL ABSTRACT

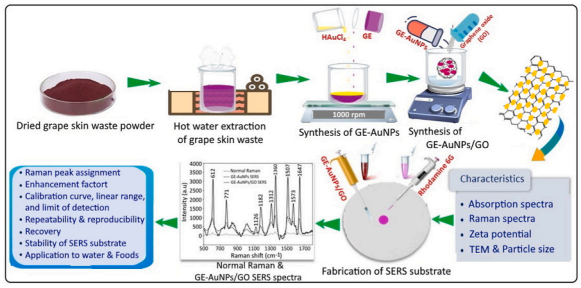

ARTICLE INFO

Handling Editor: Yasser Vasseghian

Keywords:
Grape skin
Gold nanoparticles
Graphene oxide
SERS method
Paper SERS substrate
Rhodamine 6G

ABSTRACT

Organic toxins are persistent chemicals of global concern capable of accumulating in environment and food. Surface enhanced Raman spectroscopy (SERS) is a promising technique that facilitates onsite detection of organic toxins. However, the fabrication of a SERS substrate is complicated and difficult to provide flexibility, fastness and cost-effectiveness. This study aims to develop a paper-based SERS method using grape skin-gold nanoparticles/graphene oxide (GE-AuNPs/GO) as SERS substrate and evaluate its efficiency with rhodamine 6G (Rh6G) as a model organic toxin and a real water and food contaminant. GE-AuNPs synthesized by green method using grape skin waste extract and GE-AuNPs/GO showed a surface plasmon resonance at 536 and 539 nm, particle size 18.6 and 19.5 nm, and zeta potential −44.6 and −59.7 mV, respectively. Paper-based SERS substrates were prepared by coating a hydrophobic thin-film of 30% polydimethylsiloxane solution in hexane on Whatman no. 1 filter paper, followed by drop-casting GE-AuNPs or GE-AuNPs/GO and drying. The SERS signals of Rh6G showed an enhancement factor of 5.8×10^4 for GE-AuNPs and 1.92×10^9 for GE-AuNPs/GO, implying that a combination of electromagnetic surface plasmon, charge transfer and molecular resonances may be responsible for a higher enhancement of signal by the latter. A low detection limit of 7.33×10^{-11} M in the linear range of 10^{-11}–10^{-5} M was obtained for GE-AuNPs/GO, while the relative standard deviation of repeatability and reproducibility was 9.6 and 12.6%, respectively. Paper-based GE-AuNPs/GO SERS substrate was highly

* Corresponding author. Department of Food Science, Fu Jen Catholic University, New Taipei City 24205, Taiwan.
E-mail address: 002622@mail.fju.edu.tw (B.-H. Chen).
[1] Equally contributed to this work.

https://doi.org/10.1016/j.chemosphere.2022.134702
Received 8 March 2022; Received in revised form 8 April 2022; Accepted 20 April 2022
Available online 25 April 2022

stable as <20% loss in efficiency was shown over a 60-day storage period. Application to real samples showed a high recovery of Rh6G from tap water (93.9–100.8%) as well as food samples such as red chilli powder (91.0–95.4%), red glutinous rice ball (96.6–98.3%) and tomato ketchup (98.9–102.3%) after QuEChERS extraction. Collectively, the developed paper-based GE-AuNPs/GO can be a potential substrate for sensitive onsite detection of rhodamine 6G by SERS method.

1. Introduction

Organic toxins are persistent contaminants present in food and environment which can cause detrimental health effects on humans. Many organic toxins such as toxic dyes, pesticides, polycyclic aromatic hydrocarbons (PAHs) and heterocyclic amines (HAs) appear in water and food due to human interventions, cooking and processing methods (Hung et al., 2021; Inbaraj et al., 2021a). Owing to the stringent maximum permissible limits set by the International authorities, there is an urgent need for a highly sensitive analytical method for detection of organic toxins in water and food (EU, 2011; Inbaraj et al., 2021a). Although several analytical methods employed for determination of organic toxins, such as fluorescence polarization assay and Fourier transform near-infrared spectroscopy (FT-NIR) as well as high performance liquid chromatographic and gas chromatographic methods coupled with tandem mass spectrometer (HPLC-MS/MS and GC-MS/MS) provide high sensitivity and selectivity (Singh and Mehta, 2020), they possess several drawbacks such as complicated steps, requirement of skilled personnel and difficulty to permit onsite detection. These limitations have substantially reduced their applications in developing countries.

Surface enhanced Raman spectroscopy (SERS) is a surface sensitive technique that enhances Raman signals of molecules adsorbed on metal or nanostructures (Langer et al., 2020). It is emerging as a promising method for sensitive detection of chemical and biological analytes through signal enhancement by electromagnetic (EM) and chemical (CM) mechanisms caused by localized surface plasmon resonance on metal surface (Au, Ag, Ni, and Cu) and charge transfer between metal and molecule, respectively (Li et al., 2017). Although silver nanoparticles exhibit strong SERS effect, they are quite susceptible to oxidation and/or denaturation resulting in poor stability (Wang et al., 2020a). Consequently, gold nanoparticles have become a potential alternative as SERS substrate capable of providing high stability, high surface area and strong surface plasmon resonance (Lee and Kim, 2019). In recent years, nanohybrids of metal nanoparticles with graphene nanomaterials are becoming popular as they tend to enhance Raman signals by synergistic EM and CM effects and enable effective adsorption of analytes (Nan et al., 2018; Nancy et al., 2019). Graphene oxide (GO), an oxidized form of graphene possessing several oxygen-containing functional groups (epoxy and hydroxy), is capable of enhancing Raman signals by charge transfer between GO and metal surface (chemical mechanism) and generation of localized dipole moments (Shahriari et al., 2021). GO-based metal nanohybrids can also increase surface area and dispersibility as well as exhibit fluorescence quenching effects (Kavitha et al., 2015).

Gold nanoparticles (AuNPs) synthesized by chemical methods generate toxic byproducts through usage of excess chemicals and organic solvents (Krishnaswamy et al., 2014). Instead, the environment-friendly green methods were explored for synthesis of metal nanoparticles by replacing chemicals with plant extracts, biopolymers, fungi, bacteria and enzymes (Elia et al., 2014; Lee et al., 2020). Grape, a popular fruit cultivated globally, generates a large amount of grape pomace waste after juice and wine making. More importantly, the grape skin extract contains a significant amount of bioactive compounds such as resveratrol, phenolic acid, flavonoid and proanthocyanidin, all of which can be used as both reducing and stabilizing agents for synthesis of AuNPs (González-Ballesteros et al., 2018; Inbaraj et al., 2021b). Likewise, the GO-metal nanoparticle hybrids are usually prepared by *in situ* reduction of metal salts on GO sheets (Shahriari et al., 2021). However, this synthesis method fails to provide a proper control on particle size and morphology (Huang et al., 2010). Thus, it is imperative to prepare AuNPs by adopting a green method for their subsequent conjugation with GO by a facile ligand-free synthesis method.

Conventionally, the nanostructures are fabricated on solid supports by various methods which usually involve complex fabrication methods such as electron beam lithography, physical vapor deposition, focus ion beam and electrochemical deposition (Dalla Marta et al., 2017; Lee et al., 2018). Also, the traditional solid supports such as glass and silicon are difficult to be functionalized, non-environmentally friendly and expensive. Instead, the paper-based substrates are evolving as potential replacements to conventional SERS substrates owing to their cheapness, flexibility in handling, easy functionalization and disposability as well as biodegradability (Dalla Marta et al., 2017). However, the high porosity, hygroscopic and hydrophilic nature of paper-based substrates can significantly reduce both sensitivity and reproducibility of sensors. To remedy this problem, an appropriate surface modification is necessary for paper-based SERS substrates to enhance sensitivity, repeatability and reproducibility of analytes. Several methods have been investigated to enhance the SERS signal generated by paper-based SERS substrates which include chemical growth, electrostatic adsorption, aggregation/filtration of nanoparticles, wax printing and light-induced deposition of nanoparticles (Dalla Marta et al., 2017; Lee et al., 2018). However, they usually involve complicated processes, sophisticated instruments or expensive substrate fabrication, which are difficult to provide uniform nanoparticle distribution, high reproducibility and high sensitivity.

More recently, surface modification of a filter paper by altering its hydrophilic property into hydrophobic was reported as a simple and inexpensive way to overcome these issues. However, only a few studies have been reported so far on fabricating a paper-based SERS substrate with hydrophobic surface modification. For instance, Lee et al. (2018) prepared an alkyl ketene dimer-treated hydrophobic filter paper by converting hydroxyl groups on the papers' cellulose fibers into alkyl groups, and by depositing silver nanoparticles (AgNPs) on its surface, a high reproducibility with a relative standard deviation (RSD) of 6.19% was shown for 4-aminothiophenol. In another study, the SERS signals of rhodamine 6G (Rh6G) was shown to enhance with an increased reproducibility (RSD decrease from 27 to 9%) for AgNPs deposited on a paper substrate coated twice with cellulose nanofibrils (Oh et al., 2018). In our study, we fabricated a surface-modified paper-based substrate by drop-casting polydimethylsiloxane (PDMS) on a Whatman No. 1 filter paper.

Several studies have used the xanthenic dye Rhodamine 6G (Rh6G) as a model to enhance sensitivity of organic toxins by SERS method (Wang et al., 2020a, 2020b). Besides using as a model organic toxin, the Rh6G was also used as a real contaminant in this study because of its carcinogenic nature and it is still being illegally used as a food colorant due to its low cost and high color intensity (Rajoriya et al., 2017; Xiao et al., 2014). Consequently, the developed SERS method was tested for its efficiency in environmental sample (tap water) as well as food samples (red chilli pepper powder, red glutinous rice ball and tomato ketchup). Thus, the objectives of this study were to develop an improved SERS method by using a paper-based waste grape skin extract-stabilized AuNPs/GO substrate for sensitive detection of Rh6G in water and food.

2. Materials and methods

2.1. Materials

A total of 10-kg Kyoho grape pomace was provided as a gift by a commercial vender in Xinzhuang District, New Taipei City, Taiwan. Then, the grape skin was separated manually from the pomace and freeze-dried (FD24, Chin-Min Co, Taipei, Taiwan) to obtain dried grape skin (2 kg), which was ground into fine powder and stored at −20 °C for further use. Gold (III) chloride trihydrate ($HAuCl_4{\cdot}3H_2O$) used for synthesis of AuNPs was obtained from Sigma-Aldrich (St. Louis, MO, USA). Graphite, sulfuric acid, sodium nitrate and hydrogen peroxide used for preparation of GO were also obtained from Sigma-Aldrich. Copper grid used for obtaining TEM images was obtained from Electron Microscopy Sciences (Hatfield, PA, USA). For preparation of SERS substrate, Whatman No. 1 qualitative filter papers were obtained from ADVANTEC (Tokyo, Japan), SYLGARD™ 184 Silicone Elastomer Kit from Dow Inc. (Midland, Michigan, USA), and hexane from Sigma-Aldrich. Deionized water from a Milli-Q system (Millipore Co, Bedford, MA, USA) was used for preparation of chemicals and other solutions. The real food samples including red chilli pepper powder, red glutinous rice ball and tomato ketchup were procured from a local supermarket in New Taipei City (Taiwan). For extraction of Rh6G from real food samples, the QuEChERS (quick, easy, cheap, effective, rugged and safe) extraction kit from Yo-Ho Trade Co. (New Taipei City, Taiwan) was used, with an extraction pouch containing 4 g of magnesium sulfate plus 1 g of sodium acetate, purification pouch containing 900 mg of magnesium sulfate plus 300 mg of primary secondary amine (PSA) and a ceramic homogenizer.

2.2. Extraction of grape skin extract (GE)

A method based on Baron et al. (2021) was modified and used for extraction of grape skin waste. A 1-g grape skin waste powder was mixed with 30 mL of hot water and shaken in a B601 model reciprocating water bath shaker from Firstek Scientific Co. (New Taipei City, Taiwan) at 90 °C for 1 h, followed by centrifuging at 4000 rpm for 20 min and collecting the supernatant as grape skin extract for synthesis of AuNPs.

2.3. Synthesis of AuNPs by using grape skin waste extract (GE-AuNPs)

According to a method reported by Inbaraj et al. (2020), GE-AuNPs were prepared by a green method using grape skin waste extract as both reducing and stabilizing agent. Initially, 3 mL of grape skin waste extract was heated to 85 °C for 5 min with simultaneous stirring at 1000 rpm in a hot plate. After the solution reached 85 °C, 2 mL of 5 mM $HAuCl_4{\cdot}3H_2O$ was added slowly with both heating and stirring continued until the color of solution turned to wine red (5 min), indicating the formation of GE-AuNPs. The reaction was continued for another 5 min to ensure complete reduction of gold salt to AuNPs with a total synthesis time of 15 min. The as-synthesized GE-AuNPs were then centrifuged at 9000 rpm for 30 min, followed by removing the supernatant and redispersing the GE-AuNPs in deionized water.

2.4. Synthesis of GO by modified Hummer's method

Based on a modified Hummer's method reported by Punniyakotti et al. (2021), GO was synthesized by vigorous stirring of 3 g of commercial graphite powder and 3 g of $NaNO_3$ in 100 mL of concentrated H_2SO_4 (98%) in an ice bath at 0 ± 2 °C. After complete dispersion, 12 g of $KMnO_4$ was gradually added to avoid a sudden rise in temperature, followed by stirring at 35 °C for 3 h and gradually adding 150 mL of distilled water to the container. Then, the temperature of this reaction mixture was raised to 98 ± 2 °C for 15 min and 15 mL of hydrogen peroxide (30%) added to neutralize excess $KMnO_4$. Finally, the mixture was cooled to room temperature, centrifuged at 10,000 rpm for 30 min and the precipitate washed sequentially with 1% HCl and ethanol and then dried at 60 °C for 12 h.

2.5. Synthesis of GE-AuNPs anchored GO (GE-AuNPs/GO)

A method reported by Yu et al. (2018) was used with a slight modification for the synthesis of GE-AuNPs/GO. Briefly, 1 mg mL^{-1} of GO dispersed in deionized water was mixed with GE-AuNPs at different ratios (1:1, 1:5, 1:10 and 1:20) and the mixture stirred at room temperature for 3 h at 1000 rpm with a magnetic stirrer.

2.6. Characterization of GE-AuNPs, GO and GE-AuNPs/GO

The formation of GE-AuNPs was confirmed by monitoring the typical surface plasmon resonance (SPR) peak in the absorption spectra during synthesis. Samples of $HAuCl_4{\cdot}3H_2O$ solution (5 mM), GE-AuNPs and GE-AuNPs/GO were diluted 5 times separately, after which 2 mL sample each was collected in a colorimetric tube for determination of absorbance at room temperature in the wavelength range of 200–800 nm by a Hitachi UV-VIS spectrophotometer (U1900 model, Tokyo, Japan) (Inbaraj et al., 2020, 2021b). Similarly, the formation of GO was confirmed by the typical Raman spectra obtained by a portable Raman spectrometer (ProsTrusTech Co, Ltd, Tainan, Taiwan) (Nancy et al., 2019; Baskoro et al., 2018). The surface charge of GE-AuNPs and GE-AuNPs/GO was determined by measuring the zeta potential of 5-fold diluted samples by a Horiba zeta potential analyzer (SZ100 model, Kyoto, Japan) (Inbaraj et al., 2020). Both particle size and surface morphology were determined by capturing high resolution images in a 2100 F model JOEL transmission electron microscope (Tokyo, Japan). Briefly, 20 μL of 5-fold diluted GE-AuNPs and GE-AuNPs/GO was separately dropped on a 200-mesh copper grid and allowed to stand for 1 min, followed by carefully removing the excess sample using a filter paper, drying overnight in a desiccator for imaging determination at 120 kV (Inbaraj et al., 2020, 2021b).

2.7. Fabrication of a paper-based SERS substrate

A method based on Lee and Kim (2019) was modified and used for fabrication of hydrophobic paper-based SERS substrate. Initially, a hydrophobic thin-film coating on a Whatman No.1 filter paper was optimized by mixing SYLGARD™ silicone elastomer base and curing agent (polydimethylsiloxane, PDMS) at different ratios (10:1; 10:2; 10:3; 10:4; 10:5, v/v), and the ratio of 10:1 being able to provide adequate hydrophobicity was chosen. Then, the optimized PDMS solution (10:1, v/v) was diluted with hexane at different percentages (10%, 20%, 30%, 40% and 60%) and an optimized percentage of 30% PDMS in hexane was dropped on a Whatman No.1 filter paper and cured at room temperature for 48 h. The hydrophobic paper-based SERS substrate was then prepared by drop-casting 50 μL of GE-AuNPs or GE-AuNPs/GO and drying at 60 °C in an oven 5 times on the same spot, followed by drop-casting 50 μL of Rh6G and drying by a hair-dryer 3 times on the same spot.

2.8. Raman spectrometer instrumentation

Initially, the portable Raman spectrometer from ProTrusTech Co. Ltd. (Tainan, Taiwan) equipped with a 50X Olympus microscope and complimentary metal-oxide semiconductor (COMS) detector at an excitation wavelength of 532 nm was calibrated by using a silica slide to obtain an intensity in the range from 20,000 to 30,000 arbitrary unit (a.u) at 520 cm^{-1}. Then, the hydrophobic SERS substrate fabricated with GE-AuNPs or GE-AuNPs/GO and Rh6G were exposed to a laser for 6 scans with 5 s acquisition per scan in the Raman shift range of 200–2000 cm^{-1} at a resolution of 4 cm^{-1} and averaging them to obtain a single Raman spectrum for observation of Rh6G signal enhancement by GE-AuNPs and GE-AuNPs/GO. Optimization for high Raman signal intensity was performed by adjusting several instrumental parameters

such as laser power, integration time and averaging number. For comparison, the normal Raman spectra was recorded by irradiating 10^{-1} M Rh6G solution in deionized water with laser and optimizing the instrumental parameters as described above.

2.9. Determination of enhancement factor

After obtaining both normal Raman and SERS Raman spectra, the peaks were characterized by assigning each peak to its corresponding molecular vibrations. Next, a most prominent and high-resolution peak at 1647 cm^{-1} showing high peak intensity, resolution and symmetry was chosen as a marker peak for identification and quantitation of Rh6G. The enhancement factor for Rh6G by GE-AuNPs and GE-AuNPs/GO was determined based on Rh6G concentration and Raman intensity at 1647 cm^{-1} using the equation (1) shown below (Lee et al., 2019):

$$\text{Enhancement factor} = \left(\frac{I_{SERS}}{I_{NRS}}\right) \times \left(\frac{C_{NRS}}{C_{SERS}}\right) \quad (1)$$

where, I_{NRS} and I_{SERS} are the marker peak intensity at 1647 cm^{-1} obtained from normal Raman and SERS spectra, respectively, while C_{NRS} and C_{SERS} are the corresponding concentration of Rh6G used. For comparison of enhancement factor for GE-AuNPs without and with GO, normal Raman spectra was obtained for 10^{-1} M Rh6G solution on a silica glass slide and then two separate SERS substrates were prepared for GE-AuNPs and GE-AuNPs/GO each with Rh6G concentration at 10^{-5} M and 10^{-7} M respectively, followed by obtaining the marker peak intensity at 1647 cm^{-1} from normal Raman and SERS spectra as described above for calculation of enhancement factor using the equation (1).

2.10. Preparation of calibration curve as well as determination of linear range and detection limit

A total of 7 different concentrations (10^{-11}, 10^{-10}, 10^{-9}, 10^{-8}, 10^{-7}, 10^{-6} and 10^{-5} M) of Rh6G solutions were prepared separately by diluting the stock Rh6G solution (10^{-2} M) with deionized water. Then, by adopting the same procedure as described above, the marker peak intensity at 1647 cm^{-1} was obtained at 5 random spots on GE-AuNPs/GO SERS substrate and plotted against the corresponding Rh6G concentration to prepare the calibration curve. Triplicate measurements on 3 different GE-AuNPs/GO SERS substrates for each concentration were carried out and the mean values obtained. Both linear regression equation and coefficient of determination (r^2) were obtained directly from the Microsoft Excel worksheet, while the linear range was determined based on the concentration range showing a linear response for Rh6G detection. The detection limit (DL) was obtained by dividing the standard deviation (SD) of triplicate measurements of blank noise peak obtained from GE-AuNPs/GO SERS spectra without Rh6G by the slope value (σ) from the Rh6G calibration curve using the formula shown below (Wang et al., 2020a):

$$\text{Detection limit (M)} = 3 \times \frac{SD}{\sigma} \quad (2)$$

2.11. Determination of repeatability and reproducibility

The repeatability was determined by obtaining SERS spectra at 20 random spots on the same GE-AuNPs/GO SERS substrate prepared with 10^{-5} M Rh6G, while the reproducibility determined by obtaining a total of 20 SERS spectra at 4 random spots on 5 GE-AuNPs/GO SERS substrates each. Then, the marker peak intensity at 1647 cm^{-1} was obtained from all the SERS spectra and based on the mean values, the relative standard deviation (RSD) was calculated using the equation (3) shown below (Lee and Kim, 2019; Wang et al., 2020b):

$$\text{RSD (\%)} = \left(\frac{\text{Standard deviation}}{\text{Mean}}\right) \times 100 \quad (3)$$

2.12. Stability of SERS-active GE-AuNPs/GO

The stability of freshly-made SERS-active GE-AuNPs/GO was determined by preparing GE-AuNPs/GO SERS substrate using the same procedure as shown above and obtaining a total of 54 SERS spectra for 10^{-5} M Rh6G solution from 3 random points each in 3 different GE-AuNPs/GO SERS substrates once every 10 d over a period of 60 d to examine the change in the peak intensity at 1647 cm^{-1} (Shi et al., 2018). The GE-AuNPs/GO SERS substrates were stored in a drying oven at room temperature during the storage period.

2.13. Application of GE-AuNPs/GO SERS to tap water samples

Recovery of Rh6G was determined by spiking three Rh6G concentrations (10^{-9}, 10^{-7} and 10^{-5} M) into tap water samples separately, followed by preparing GE-AuNPs/GO SERS substrate as described above and obtaining a total of 15 SERS spectra from 5 random spots for each Rh6G concentration. Then, based on the mean peak intensity at 1647 cm^{-1} and their corresponding Rh6G concentration obtained from the calibration curve, the recovery and RSD values were calculated by using the formula shown in equations (4) and (3), respectively (Wang et al., 2020a, 2020b):

$$\text{Recovery (\%)} = \left(\frac{\text{Amount after SERS} - \text{Original amount before SERS}}{\text{Spiked amount}}\right) \times 100 \quad (4)$$

2.14. Application of GE-AuNPs/GO SERS to food samples

The developed GE-AuNPs/GO SERS method was applied to three food samples, namely, red chilli pepper powder, red glutinous rice ball and tomato ketchup. Initially, the food samples were extracted based on two QuEChERS methods reported by Brady and Burgess (2015) and Adam et al. (2018) with some modifications. A 2-g sample was weighed into a 50-mL centrifuge tube separately and homogenized with 10 mL deionized water by vortexing with a ceramic stone for 1 min. Then, 10 mL of 1% acetic acid in acetonitrile was added and vortexed again for 1 min, followed by adding QuEChERS extraction powder containing 4 g of magnesium sulfate and 1 g of sodium acetate, ultrasonicating for 10 min and centrifuging at 4000 rpm at 4 °C for 10 min. The supernatant (6 mL) was collected and poured into a 15-mL centrifuge tube containing purification powder (900 mg magnesium sulfate and 100 mg PSA). The mixture was vortexed for 1 min, centrifuged at 4000 rpm at 4 °C for 8 min and the supernatant (1 mL) collected for Rh6G analysis by GE-AuNPs/GO SERS method. The matrix effect for Rh6G analysis in the three food sample extracts was determined by preparing the matrix-matched calibration curves using 7 different Rh6G concentrations (10^{-11}, 10^{-10}, 10^{-9}, 10^{-8}, 10^{-7}, 10^{-6} and 10^{-5} M) separately in the aqueous extracts of red chilli pepper powder, red glutinous rice ball and tomato ketchup. Then, the slopes of the standard calibration curves and matrix-matched calibration curves obtained for each food sample were compared to estimate the matrix effect caused by signal enhancement or suppression (Brady and Burgess, 2015).

For determination of Rh6G recovery, a method reported by Brady and Burgess (2015) was modified. Briefly, 1 mL of three Rh6G concentrations (10^{-9}, 10^{-7} and 10^{-5} M) each were added separately to homogenized food samples, after which the mixture was subjected to QuEChERS extraction as described above. Next, the food samples extracts were separately drop-casted on a GE-AuNPs/GO SERS substrate and a total of 27 SERS spectra was obtained from 3 random spots for each Rh6G concentration in three food samples extracts. Based on the marker peak intensity at 1647 cm^{-1} and corresponding Rh6G concentration obtained from the calibration curves, the recovery of Rh6G from food samples was determined using the equation (4).

3. Results and discussion

3.1. Rhodamine 6G as a model for organic toxin as well as real water and food contaminant

In recent years, the contamination of food by environmental organic toxins has become a vital issue raising concerns on food safety worldwide. Consequently, there is an urgent need to develop a simple and sensitive analytical method which can be used both indoor and onsite detection of organic toxins in environmental and food samples. Owing to the fact that the colored dyes are strong indicators of organic contamination, Rh6G, a pink-colored cationic polar dye with a rigid heterocyclic structure belonging to xanthene family, was used as a model dye for evaluating the SERS method developed in this study for detection of organic toxins (Pino et al., 2020).

Besides being a model organic toxin, Rh6G was also used as a real contaminant in this study for enhancement of sensitivity by the developed SERS method. Obviously, Rh6G is widely used in various fields including textiles, plastics, biotechnology, food and cosmetic industries. Especially, the use of Rh6G for food coloring has raised concerns owing to its carcinogenicity as well as reproductive and developmental toxicity (Rajoriya et al., 2017; Xiao et al., 2014). Although banned in many countries, it is still used illegally due to its low cost and visually attractive color (Zhou et al., 2021). Thus, the developed SERS method can aid detection of xanthene dyes like Rhodamine 6G in environmental samples as well as in food commodities. Figure S1 shows the molecular structure of rhodamine 6G and Table S1 summarizes some of its identification and physicochemical data.

3.2. Synthesis of GE-AuNPs, GO and GE-AuNPs/GO

AuNPs was synthesized by a green method by replacing a reducing agent trisodium citrate dihydrate frequently used in the chemical reduction method with a grape skin extract. Among the various green materials, the plant extracts containing high level of antioxidant compounds are most often favored as reducing and/or capping agents (Can, 2020; Castillo-Henríquez et al. (2020). For example, Krishnaswamy et al. (2014) have used grape skin, stalk and seeds separately for synthesis of AuNPs, reporting that catechin as well as oligomeric and polymeric proanthocyanidins were mainly responsible for reducing gold salt to AuNPs. In a later study, González-Ballesteros et al. (2018) demonstrated that the waste grape pomace possessed high total phenolic content and DPPH antioxidant activity with a sufficiently high reducing power for synthesis of AuNPs. This phenomenon can be attributed to the presence of phenolic acids and flavonoids as well as proanthocyanidins containing a high proportion of hydroxy groups in aromatic rings. More recently, Inbaraj et al. (2021b) have synthesized AuNPs by using resveratrol standard, a non-flavonoid polyphenol abundant in grape skin containing 3 hydroxyl groups, for application in an anti-pancreas cancer study. Also, in a study dealing with the development of an analytical method for determination of resveratrol and related stilbenes in grape skin, Hua et al. (2021) reported that 5 resveratrol and related stilbenes containing 2, 3 or 5 hydroxy groups were present in grape skin. Thus, in this study, an aqueous extract from grape skin waste was used for subsequent experiments.

Various synthesis conditions such as gold salt concentration, extract concentration, temperature and pH can have a great impact on size, shape and surface charge of nanoparticles. The higher the concentration of gold salt and extract, the larger the particle size and the higher the irregularity of shape (Can, 2020; Lee et al., 2020). For instance, following a rise in concentration of *Lantana camara* Linn leaf extract from 100 to 500 mg/L, the size of AuNPs was shown to increase from 6 to 100 nm (Dash et al., 2014). A similar outcome of increased particle size was observed upon raising the reaction time and temperature (Yeh et al., 2012). Also, a rise in temperature as well as the extract possessing high capability to reduce gold salt to AuNPs was reported to decrease the reaction time (Lee et al., 2017). Therefore, we optimized the concentration of gold salt ($HAuCl_4$) and grape skin extract as well as their ratio to be 5 mM, 0.3% (1 g grape skin extract in 30 mL) and 1:1.5 (v/v), respectively. In addition, a reaction temperature of 85 °C and reaction time of 15 min was found to be optimal for complete reduction of gold salt to AuNPs. However, in our previous study, a gold salt (5 mM)/resveratrol (5 mM)/water ratio of 2:1:2 (v/v/v), reaction temperature of 40 °C and reaction time of 20 min was reported to be optimal for synthesis of resveratrol AuNPs (Inbaraj et al., 2021b). Apparently, the difference in synthesis conditions can be attributed to the use of pure resveratrol standard in our previous study as compared to grape skin extract used in this study.

Furthermore, for synthesis of GO, a popular Hummer's method involving a mixture of concentrated sulfuric acid, sodium nitrite and potassium permanganate was adopted. Three main stages of this method include (1) intercalation of stacked graphite layers at low temperature (<5 °C), (2) oxidation of intercalated graphite layers at medium temperature (35 °C) and (3) hydrolysis of products at high temperature (98 °C) (Shahriari et al., 2021). Then, GE-AuNPs/GO was synthesized by a ligand-free method as it is difficult to control size and morphology of metal-GO nanohybrids prepared by the *in situ* reduction method. Based on our method, GE-AuNPs were anchored on GO through π-π, electrostatic and van der Waals interactions (non-covalent bonding) as well as distribution of AuNPs on defects or wrinkles on GO surface (Shahriari et al., 2021). Among various ratios of GO and GE-AuNPs (1:1, 1:5, 1:10 and 1:20) tested for synthesis of GE-AuNPs/GO, an optimal ratio of 1:10 was chosen in our study based on a stronger interaction and better dispersion of GE-AuNPs on GO sheet as shown in TEM images accompanied by a greater enhancement of Raman signals.

3.3. Characterization of GE-AuNPs, GO and GE-AuNPs/GO

As gold in nanoform generate a typical SPR around 520 nm, the formation of GE-AuNPs was monitored by measuring the SPR peak absorption. Compared to only gold (III) chloride trihydrate solution and GO, the appearance of SPR peak at 536 nm for GE-AuNPs and 539 nm for GE-AuNPS/GO revealed a successful formation of AuNPs by using grape skin extract (Fig. 1A). Similar SPR peak absorption (536–538 nm) was reported for AuNPs synthesized separately by using grape skin, seed and stalk extracts (Krishnaswamy et al., 2014), while that synthesized by grape pomace showed a higher value of 547 nm, probably because of using the extract from a combination of grape skin, seed and stem in grape pomace (González-Ballesteros et al., 2018).

Likewise, the successful formation of GO was confirmed by two typical Raman peaks at 1345 cm^{-1} and 1582 cm^{-1} for both GO and GE-AuNPs/GO, which is assigned to D and G peaks signifying sp^3 and sp^2 hybridized bonding on carbon in GO (Fig. 1B) (Baskoro et al., 2018). The D peak also indicated defects-induced disorder on the sp^2 hybridized hexagonal sheet of carbon caused by oxidation of graphite (Nancy et al., 2019). Several studies have also reported D and G peaks for AuNPs/GO (1330 and 1600 cm^{-1}) (Huang et al., 2010) and AgNPs/GO/AuNPs (1336 and 1598 cm^{-1}) (Zhang et al., 2017). The presence of these marker Raman peaks in our study for both GO and GE-AuNPs/GO suggested that the GO structure remained unaffected after anchoring of GE-AuNPs on GO surface. The D-peak intensity was relatively higher compared to G-peak implying that the original sp^2 hybridized carbon bonds were broken due to oxidation of graphite resulting in the formation of sp^3 hybridized carbon bonds in GO. Moreover, a higher intensity ratio of D peak to G peak for GE-AuNPs/GO (1.06) compared to GO (0.92) revealed a successful anchoring of GE-AuNPs on GO surface. An analogue trend in the intensity ratio of D/G peak was also reported by Nancy et al. (2019) for GO (0.89) obtained by a modified Hummer's method and AuNPs-GO (1.09) by an in-situ laser ablation method.

Zeta potential, a useful indicator of nanoparticle stability in colloidal form (>+30 to <−30 mV), was determined to be −44.6 mV for GE-AuNPs, −64.9 mV for GO and −59.7 mV for GE-AuNPs/GO, implying

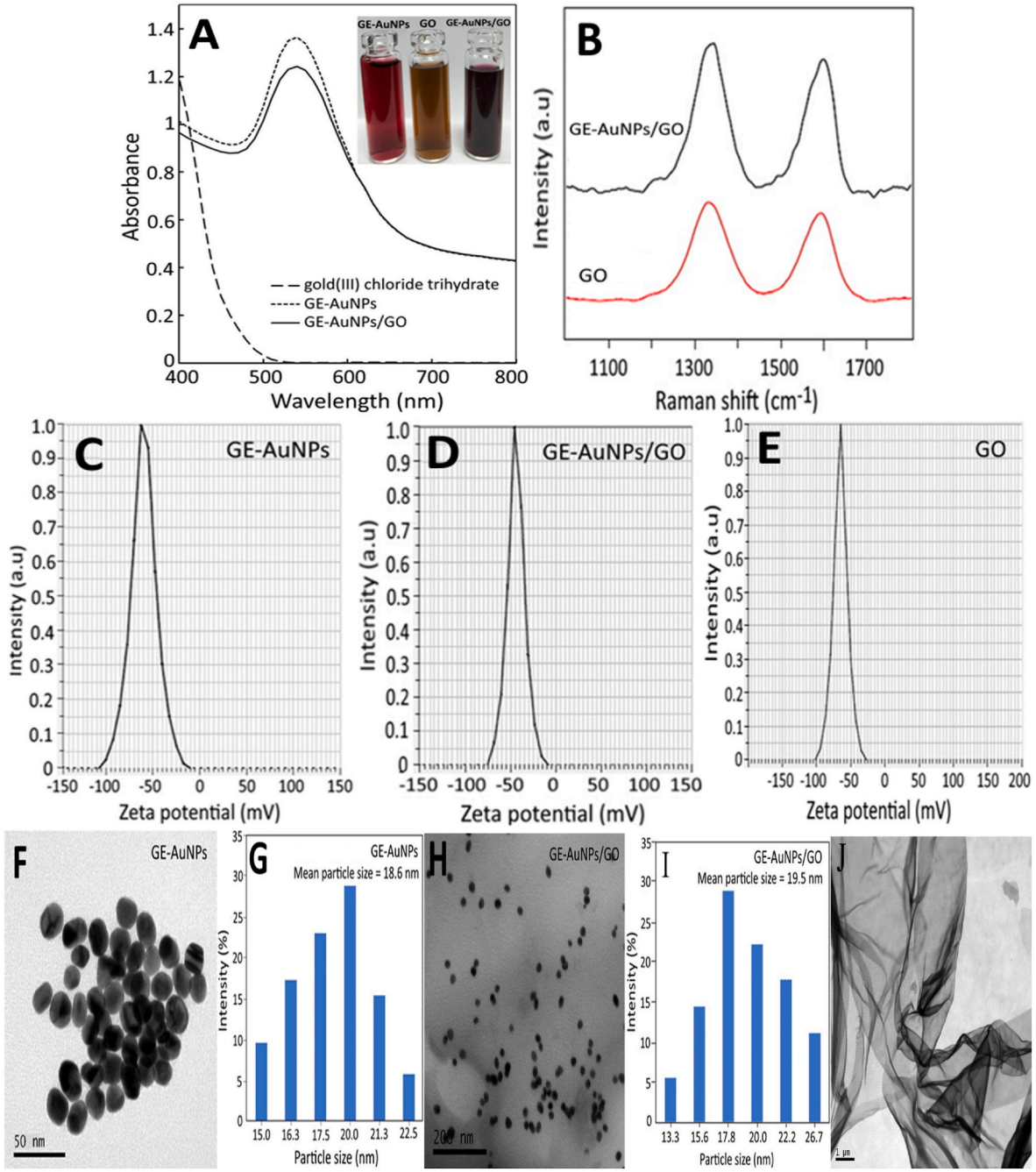

Fig. 1. Characterization of as-synthesized GE-AuNPs, GO and GE-AuNPs/GO. 1 A, absorption spectra of gold (III) chloride trihydrate, GE-AuNPs and GE-AuNPs/GO along with an inset showing the appearance of as-synthesized GE-AuNPs, GO and GE-AuNPs/GO; 1 B, Raman spectra of GO and GE-AuNPs/GO; 1C-E, zeta potential values for GE-AuNPs (1C), GE-AuNPs/GO (1D) and GO (1 E); 1 F-G, TEM image (1 F) and particle size distribution (1G) of GE-AuNPs; 1H–I, TEM image (1H) and particle size distribution (1I) of GE-AuNPs/GO; 1 J, TEM image of GO. GE-AuNPs, grape skin extract-stabilized gold nanoparticles; GO, graphene oxide; GE-AuNPs/GO, grape skin extract-stabilized gold nanoparticles anchored on graphene oxide; TEM, transmission electron microscopy. (For interpretation of the references to color in this figure legend, the reader is referred to the Web version of this article.)

a high stability of as-synthesized nanoparticles (Fig. 2C–E). Furthermore, a shift in zeta potential value (−59.7 mV) after anchoring GE-AuNPs on GO in our study confirms the effective interaction of GE-AuNPs with GO and the stability remained unaffected upon anchoring of GO onto GE-AuNPs. The TEM images depicted the spherical shape of GE-AuNPs (Fig. 1F) and GE-AuNPs/GO (Fig. 1H) along with the particle size distribution histogram (Fig. 1G, I) showing the mean particle size (18.6 nm and 19.5 nm) determined directly from the images. More specifically, the GE-AuNPs were shown to be well dispersed on the grey-colored GO sheet as evident from Fig. 1H. A relatively larger particle size of 20 nm and 40 nm was reported for AuNPs in two different AuNPs/GO samples by Huang et al. (2010). The TEM image of GO nanosheet was also shown in Fig. 1J.

3.4. Normal Raman and SERS spectral analysis of Rh6G

A paper-based SERS substrate was prepared by developing a hydrophobic thin film on Whatman No.1 filter paper with an optimized 10:1 ratio of SYLGARD™ silicone elastomer base to PDMS curing agent and an optimized 30% PDMS solution in hexane as described above.

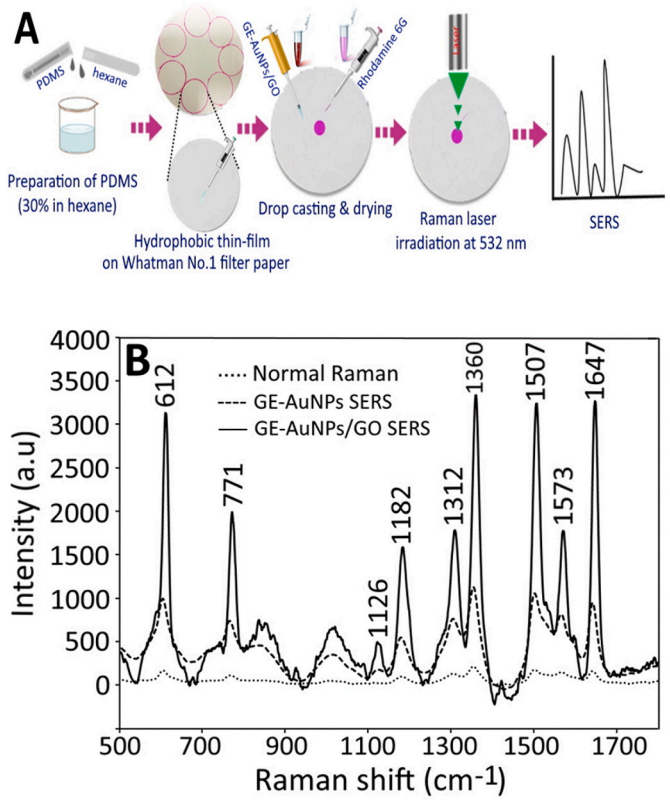

Fig. 2. A schematic diagram showing the fabrication steps for preparation of hydrophobic filter paper-based GE-AuNPs and GE-AuNPs/GO SERS substrates (A) as well as Normal Raman spectra with 10^{-1} M Rh6G solution on silica glass slide, SERS spectra with 10^{-5} M Rh6G on GE-AuNPs SERS substrate and SERS spectra with 10^{-7} M Rh6G on GE-AuNPs/GO SERS substrate (B). The fabrication steps illustrated in Fig. 2A includes preparation of 30% PDMS solution in hexane, followed by developing a hydrophobic thin-film of PDMS on several 1.5 cm circles made in a Whatman No. 1 filter paper, drop-casting 50 μL of GE-AuNPs/GO and drying at 60 °C in an oven 5 times on the same spot, drop-casting 50 μL of Rh6G and drying by a hair-dryer 3 times on the same spot and finally irradiating with Ramen laser at 532 nm for measuring the SERS spectra. GE-AuNPs, grape skin extract-stabilized gold nanoparticles; GE-AuNPs/GO, grape skin extract-stabilized gold nanoparticles anchored on graphene oxide; SERS, surface enhanced Raman scattering; PDMS, polydimethylsiloxane; Rh6G, rhodamine 6G. (For interpretation of the references to color in this figure legend, the reader is referred to the Web version of this article.)

Then, GE-AuNPs/GO and Rh6G were sequentially drop-casted and dried on the hydrophobic paper for SERS analysis. Fig. 2A shows a schematic diagram illustrating the fabrication steps involved in preparation of paper-based GE-AuNPs and GE-AuNPS/GO SERS substrates. Initially, a normal Raman spectrum was measured by using 10^{-1} M Rh6G solution and compared with SERS spectra obtained by dropping 10^{-5} M Rh6G solution onto GE-AuNPs SERS substrate or 10^{-7} M Rh6G on GE-AuNPs/GO SERS substrate (Fig. 2B). The peak at 612 cm^{-1} was attributed to in-plane C–C–C bending vibrations in xanthene ring, while those at 771, 1126 and 1182 cm^{-1} were assigned to C–H bending vibrations in xanthene or phenyl ring. On the other hand, the peaks at 1312, 1360, 1507, 1573 and 1647 cm^{-1} were due to the symmetric modes of in-plane C–C stretching vibrations in xanthene or phenyl ring. All the peaks assignments were summarized in Table S2, which conformed well with that reported by Kavitha et al. (2015). Based on the peak symmetry, intensity and resolution, the peak at 1647 cm^{-1} was chosen as a marker peak to estimate the Raman signal enhancement efficiency, evaluate the validation parameters and obtain quantitation data for detection of Rh6G in water and food samples by the developed SERS substrates.

Compared to normal Raman spectra for 10^{-1} M Rh6G, the intensity of marker peak 1647 cm^{-1} in SERS spectra was enhanced by 5.6- and 19.6-fold for GE-AuNPs and GE-AuNPs/GO, respectively (Fig. 2B) and the enhancement factor calculated by using the equation (1) was 5.76×10^4 and 1.96×10^7, implying that the GE-AuNPs and GE-AuNPs/GO SERS substrates can provide higher sensitivity in Rh6G detection than the normal Raman spectral analysis. Also, compared to GE-AuNPs, the anchoring of GE-AuNPs on GO was shown to substantially increase the peak intensity of Rh6G and thus GE-AuNPs/GO was chosen for further study. For comparison, the enhancement factors shown above were determined at a Rh6G concentration of 10^{-5} M for GE-AuNPs and 10^{-7} M for GE-AuNPs/GO. However, the actual enhancement factor by SERS spectral analysis can be estimated based on the marker peak intensity (1647 cm^{-1}) obtained for the lowest Rh6G concentration in the linear range as shown in the following section.

3.5. Determination of linear range, detection limit and enhancement factor

A calibration curve was prepared by drop-casting 7 different Rh6G concentrations (10^{-11}–10^{-5} M) separately on GE-AuNPs/GO SERS substrate (Fig. 3A). Following a rise in Rh6G concentration, the intensity

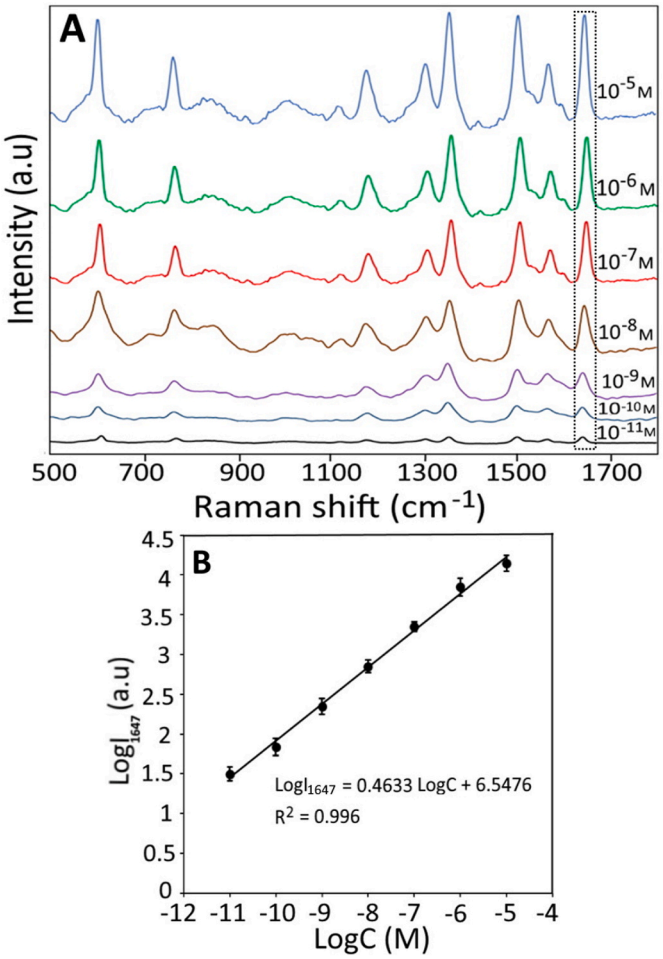

Fig. 3. GE-AuNPs/GO SERS spectra of Rh6G at different concentrations (10^{-11}–10^{-5} M) (A) and the calibration curve prepared using the marker peak intensity at 1647 cm^{-1} (B). Each data point in Fig. 4B is the mean value of triplicate measurements. GE-AuNPs/GO, grape skin extract-stabilized gold nanoparticles anchored on graphene oxide; SERS, surface enhanced Raman scattering; Rh6G, rhodamine 6G; a. u, arbitrary unit; logC, logarithm of Rh6G concentration; $logI_{1647}$, logarithm of peak intensity at 1647 cm^{-1}. (For interpretation of the references to color in this figure legend, the reader is referred to the Web version of this article.)

of all the characteristic Rh6G peaks increased and by plotting $LogI_{1647}$ versus LogC, a linear relationship was shown in the Rh6G concentration ranging from 10^{-11}–10^{-5} M (Fig. 3B), suggesting that the detector response for the Rh6G concentration was linear in this range. The error bars in Fig. 3B represent standard deviation of triplicate measurements on three different GE-AuNPs/GO SERS substrates. The linear regression equation and coefficient of determination (R^2) obtained from the Microsoft Excel software were $LogI_{1647} = 0.4633LogC + 6.5476$ and 0.996 respectively, where $LogI_{1647}$ is the logarithm of SERS peak intensity at 1647 cm^{-1} and LogC is the logarithm of Rh6G concentration. Also, based on the formula shown in the equation (2), the detection limit was determined to be 7.33×10^{-11} M. For evaluation of enhancement efficiency of Rh6G by GE-AuNPs/GO SERS substrate, the actual enhancement factor was estimated by substituting the marker peak intensity at 1647 cm^{-1} from normal Raman and SERS spectra along with their corresponding Rh6G concentrations (10^{-1} M for normal Raman and 10^{-11} M for SERS) in equation (1). By using the peak intensity (1647 cm^{-1}) obtained for the lowest Rh6G concentration in the linear range (10^{-11} to 10^{-5} M), the enhancement factor was calculated to be 1.92×10^9, demonstrating that a large Raman signal enhancement was attained by using the paper-based GE-AuNPs/GO SERS substrate. Several published reports on various metal nanoparticles-based SERS substrates used for detection of Rh6G showed that the linear range, detection limit and enhancement factor ranged from 10^{-12}–10^{-3} M, 1×10^{-12}–$1x10^{-7}$ M and 9.2×10^5–7.3×10^8, respectively (Table 1) (Bai et al., 2018; Chiang et al., 2017; Hamzah and Humud, 2021; Lee and Kim, 2019; Ouhibi et al., 2020; Shi et al., 2018; Wang et al., 2020a, 2020b; Zhang et al., 2017). In our study, a comparable linear range (10^{-11}–10^{-5} M) and detection limit (7.33×10^{-11} M), as well as a relatively higher enhancement factor (1.92×10^9) was obtained, demonstrating again that an efficient paper-based GE-AuNPs/GO SERS substrate exhibiting high Raman signal enhancement was successfully prepared.

Table 1
Linear range, detection limit and enhancement factor for detection of Rh6G by SERS substrates in this study and several other studies.

SERS substrate	Linear range (M)	Detection limit (M)	Enhancement factor	Reference
AuNPs/1 LG/AuNPs	10^{-10} to 10^{-5}	1×10^{-9}	2.5×10^8	Zhao et al. (2014)
AuNPs/PU-PAZ	10^{-8} to 10^{-5}	1×10^{-8}	9.2×10^5	Chiang et al. (2017)
AuNIs/DW	10^{-7} to 10^{-3}	1×10^{-7}	2.8×10^6	Shi et al. (2018)
Cu–Ag layered film	10^{-9} to 10^{-5}	1×10^{-9}	7.3×10^8	Bai et al. (2018)
AuNPs@GO	10^{-8} to 10^{-3}	1×10^{-8}	–	Lee and Kim (2019)
SiNWs	10^{-11} to 10^{-6}	1×10^{-11}	0.6×10^6	Ouhibi et al. (2020)
ER Nano-Au film	10^{-9} to 10^{-5}	7.1×10^{-11}	2.5×10^8	Wang et al. (2020a)
AuA-pMIP	10^{-10} to 10^{-4}	1×10^{-10}	1.2×10^6	Wang et al. (2020b)
AgNWs@AgNPs	10^{-12} to 10^{-6}	1×10^{-12}	2.3×10^7	Hamzah and Humud (2021)
AgNWs@PDA@AgNPs	10^{-12} to 10^{-6}	1×10^{-12}	2.5×10^7	Hamzah and Humud (2021)
GE-AuNPs/GO	10^{-11} to 10^{-5}	7.3×10^{-11}	1.9×10^9	This study

SERS, surface enhanced Raman scattering; Rh6G, rhodamine 6G; AuNPs/1 LG/AuNPs, gold nanoparticles sandwiched 1-layered graphene; AuNPs/PU-PAZ, gold nanoparticles immobilized honeycomb-like self-assembled polyurethane-*co*-azetidine-2,4-dione polymer; AuNIs/DW, gold nanoislands on dragonfly wings; Cu–Ag layered thin film; SiNWs, silicon nanowires; AuNPs@GO, gold nanoparticles arranged on GO flakes; ER-nano-Au film, electrochemical roughened nano-gold film; AuA-pMIP, porous molecularly imprinted polymer sandwiched in gold nanoparticle array; AgNWs, silver nanowires; AgNPs, silver nanoparticles; PDA, polydopamine; GE-AuNPs/GO, grape skin extract-stabilized gold nanoparticles anchored on graphene oxide.

Some recent studies have shown that AuNPs/GO nanohybrids are excellent SERS substrates capable of enhancing Raman signals for highly sensitive detection of analytes (Huang et al., 2010; Wang et al., 2020a; Zhang et al., 2017). The Raman signal enhancement by these hybrid materials can be attributed to a combination of several mechanisms including electromagnetic, chemical and charge transfer as well as molecular resonances and synergistic electromagnetic–charge transfer between AuNPs and GO (Kavitha et al., 2015; Lee et al., 2019). The GE-AuNPs showed an enhancement factor of 5.76×10^4 for detection of Rh6G, which should be due to collective oscillations of free electrons on AuNPs surface and charge transfer electronic coupling between AuNPs and Rh6G molecule along with molecular resonances due to vibronic coupling in Rh6G molecule (Wang et al., 2020a, 2020b). Nevertheless, by anchoring GE-AuNPs on GO, a further enhancement of the Raman signals can occur through synergistic effect between AuNPs and GO.

Upon anchoring GE-AuNPs on GO, the Raman signals were greatly enhanced with an enhancement factor of 1.92×10^9 shown for GE-AuNPs/GO. Obviously, in the presence of GO, a predominant charge transfer due to electronic coupling can occur between GE-AuNPs and GO. More specifically, when GO interacts with AuNPs, it gains electron density causing a shift in fermi level due to formation of charge transfer complexes between GO and AuNPs (Shahriari et al., 2021). Also, the interaction of ring structures between GO and Rh6G through π-π stacking generates electronic and vibrational excitations during laser irradiation, providing further enhancement in Raman signals (Huang et al., 2010; Nan et al., 2018). Such combined excitations enable reduction in the fluorescence signal produced from Rh6G under laser exposure (Lee and Kim, 2019). Also, GO itself can further contribute to the local electric field during laser irradiation through generating local dipole moments because of presence of sp^2-hybridized carbons and highly electronegative oxygen atoms (Shahriari et al., 2021). Thus, the Raman signal enhancement by GE-AuNPs/GO for detection of Rh6G can be due to the combined effects of electromagnetic surface plasmon, charge transfer and molecular vibronic coupling resonances. Moreover, the fabrication of GE-AuNPs/GO on the PDMS-modified paper-based substrate can impart high repeatability (uniformity in GE-AuNPs/GO deposition within a SERS substrate) and reproducibility to the developed SERS method by reducing the porosity and surface roughness as well as providing adequate hydrophobicity (Dalla Marta et al., 2017; Lee and Kim, 2019). These surface characteristics can facilitate uniform surface deposition of GE-AuNPs/GO and confine them to a small contact area on the paper surface for increased sensitivity. Moreover, unlike solid substrates, paper-based substrates are biodegradable and easily disposable and the PDMS used for making hydrophobic thin film on filter paper is inert, non-toxic and non-flammable. They also enable onsite detection of toxins more convenient and flexible, given the fact that the technology development made Raman spectrometers available as portable and hand-held forms.

3.6. Repeatability, reproducibility and stability evaluation

The repeatability and reproducibility are the key parameters for precision evaluation of quantitative analysis by SERS. Fig. 4A shows the change in marker peak intensity at 1647 cm^{-1} collected at 20 random sites on the same GE-AuNPs/GO prepared with 10^{-5} M Rh6G solution, with a RSD value of 9.6% being shown. This finding demonstrated that the GE-AuNPs/GO SERS substrate was successfully prepared with high uniformity caused by high dispersion of GE-AuNPs/GO on a hydrophobic paper. Similarly, no significant change in 1647 cm^{-1} peak intensity occurred among 20 random points collected 4 each from 5

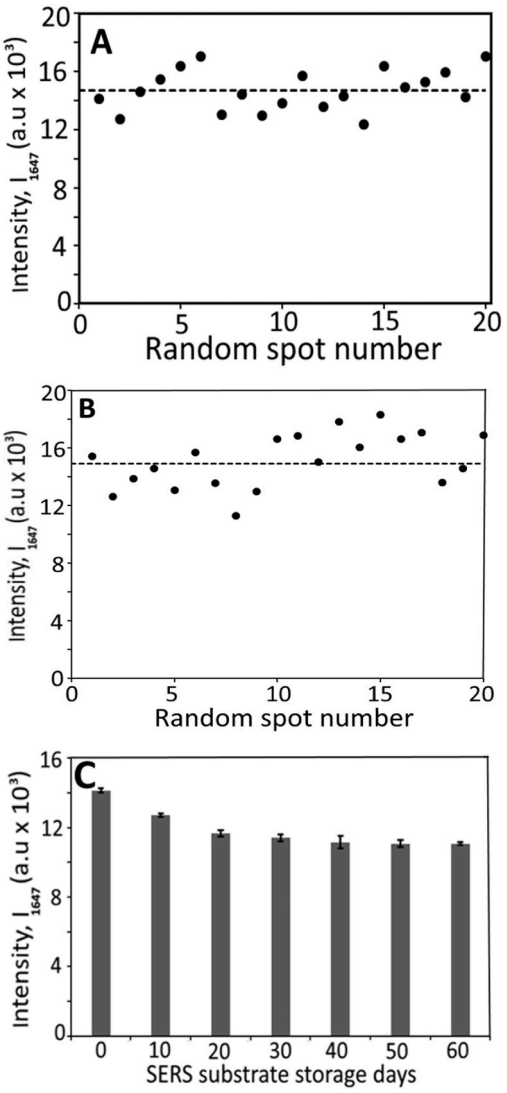

Fig. 4. Repeatability (A), reproducibility (B) and stability data (C) for Rh6G detection by GE-AuNPs/GO SERS method. Repeatability was based on 20 random points obtained from the same GE-AuNPs/GO SERS substrate, while reproducibility was based on 20 random points with 4 obtained from 5 different GE-AuNPs/GO SERS substrates each. For stability study, 9 SERS spectra were obtained from 3 random points each in 3 different GE-AuNPs/GO substrates once every 10 d over a period of 60 d. All the three studies were done using 10^{-5} M Rh6G solution. GE-AuNPs/GO, grape skin extract-stabilized gold nanoparticles anchored on graphene oxide; SERS, surface enhanced Raman scattering; Rh6G, rhodamine 6G; a. u, arbitrary unit; I_{1647}, peak intensity at 1647 cm^{-1}.

different GE-AuNPs/GO SERS substrates prepared with 10^{-5} M Rh6G solution under the same conditions (Fig. 4B). The variation in measured peak intensities yielded a RSD value of 12.6%, implying that a high reproducibility in Rh6G detection by our GE-AuNPs/GO SERS method was attained. In several previous studies a comparable repeatability (11%) and reproducibility (6.9%) was reported for nano-Au film (Wang et al., 2020a), while a reproducibility value of 8.92% and 6.22% was shown respectively for SERS substrates Au nanoislands/dragonfly wings (Shi et al., 2018) and porous molecularly imprinted polymer sandwiched AuNPs array (AuA-pMIP) (Wang et al., 2020b).

In addition, the SERS substrate needs to be evaluated for its stability during storage. Thus, a long-term stability of GE-AuNPs/GO SERS substrate for Rh6G (10^{-5} M) detection was determined over a 60-day storage period. It is evident from Fig. 4C that a 10% loss in peak intensity in first 10 d occurred, but increased to 17.5% after 20 d and 19.2% after 30 d. However, after 30 d, there was no significant change in peak intensity until 60 d, indicating that the GE-AuNPs/GO substrate possessed a high stability for SERS detection. The error bars shown in Fig. 4C represent the standard deviation of 9 SERS spectral measurements obtained from 3 random positions in 3 GE-AuNPs/GO substrates. Comparatively, in two different previous studies, a loss in SERS efficiency of 26.5% and 12.9% for Rh6G detection was shown during storage of Au nanoislands/dragonfly wings (Shi et al., 2018) and electrochemically roughened nano Au-film (Wang et al., 2020a) over a period of 60 and 70 d, respectively. The variation in stability can be due to the difference in SERS substrate preparation, Rh6G concentration and marker peak intensity used for obtaining SERS spectra. In our study, by taking into account the simplicity of GE-AuNPs/GO SERS substrate preparation, the 20% loss in efficiency over an initial period of 30 d can be deemed acceptable. Also, the high stability of GE-AuNPs/GO SERS substrate confirms that AuNPs and their anchoring with GO can provide high oxidative and mechanical stability for SERS application.

3.7. Application of GE-AuNPs/GO SERS to tap water samples

The developed GE-AuNPs/GO SERS method was applied to tap water samples and recovery was determined for evaluating accuracy of quantitative analysis. Table 2 shows the recovery data obtained by spiking three Rh6G concentrations (10^{-9}, 10^{-7} and 10^{-5} M) separately into tap water samples and drop-casting on GE-AuNPs/GO SERS substrates. Both recovery and RSD values obtained for different Rh6G concentrations were 94% and 6.8% for 10^{-9} M, 100.8% and 4.6% for

Table 2
Recovery of Rh6G spiked at 3 different concentrations into tap water as well as 3 food samples and analyzed by GE-AuNPs/GO SERS method after QuEChERS extraction.

Sample	Rh6G concentration (M)		Recovery (%)[c]	RSD (%)[d]
	Added	Detected		
Tap water[a]	1×10^{-9}	0.94×10^{-9}	93.91 ± 6.35	6.77
	1×10^{-7}	1.01×10^{-7}	100.82 ± 4.59	4.55
	1×10^{-5}	0.95×10^{-5}	94.69 ± 7.25	7.66
Red chilli pepper powder[a,b]	1×10^{-9}	0.95×10^{-9}	95.43 ± 6.90	7.24
	1×10^{-7}	0.92×10^{-7}	91.58 ± 2.21	2.41
	1×10^{-5}	0.91×10^{-5}	90.98 ± 7.58	8.33
Red glutinous rice ball[a,b]	1×10^{-9}	0.98×10^{-9}	98.32 ± 7.56	7.69
	1×10^{-7}	0.97×10^{-7}	96.62 ± 8.67	8.98
	1×10^{-5}	0.98×10^{-5}	97.51 ± 6.12	6.27
Tomato ketchup[a,b]	1×10^{-9}	1.01×10^{-9}	100.54 ± 3.77	3.75
	1×10^{-7}	1.02×10^{-7}	102.32 ± 4.47	4.37
	1×10^{-5}	0.98×10^{-5}	98.90 ± 8.26	8.35

SERS, surface enhanced Raman scattering; Rh6G, rhodamine 6G; GE-AuNPs/GO, grape skin extract-stabilized gold nanoparticles anchored on graphene oxide; QuEChERS, quick, easy, cheap, effective, rugged and safe.

[a] No Rh6G was detected originally in water and food samples.

[b] All the three food samples were spiked with three different Rh6G concentrations separately, followed by QuEChERS extraction and detection by GE-AuNPs/GO SERS method.

[c] The recovery was calculated using the formula, recovery (%) = ((amount after SERS-original amount before SERS)/spiked amount) x 100.

[d] The relative standard deviation (RSD) was calculated using the formula, RSD (%) = (standard deviation/mean) x 100.

10^{-7} M and 94.7% and 7.7% for 10^{-5} M, respectively, demonstrating that the developed GE-AuNPs/GO SERS method is accurate for application to environmental samples. A similar outcome was shown for electrochemically roughened nano Au-film, with a Rh6G recovery of 96–98% (RSD, 9%) being shown for tap water (Wang et al., 2020a).

3.8. Application of GE-AuNPs/GO SERS to real food samples

The application of GE-AuNPs/GO SERS method to three food samples including red chilli pepper powder, red glutinous rice ball and tomato ketchup was evaluated by extraction using a QuEChERS method as described above. It is worth mentioning that QuEChERS is a dispersive solid-phase extraction (dSPE) method that involves three major steps of liquid–liquid partitioning using solvents such as acetonitrile, salting-out extraction/phase separation using salt mixture and purification by dSPE sorbent mixtures (Hua et al., 2021). This versatile method is employed in a wide variety of sample matrices and possesses several advantages such as the environment- and user-friendly green approach, low solvent consumption, less lab space and washing requirement, low-sorbent usage, efficient dispersive sorbent interaction with matrix components for enhancement of signal-to-noise ratio, less sample pretreatment time with low-cost and high sample throughput (Hua et al., 2021). The sequential steps involved in extraction of Rh6G from food samples by QuEChERS method are shown in Fig. 5A. After plotting a matrix-matched calibration curve for each food sample extract in the Rh6G concentration from 10^{-11}–10^{-5} M, the slope value was compared with that of the standard calibration curve prepared in deionized water. A slope ratio close to 1 was obtained for red chilli pepper powder (0.95), red glutinous rice ball (0.98) and tomato ketchup (1.03), revealing an absence of matrix effect in Rh6G analysis in food samples. A slope ratio of 1, >1 and < 1 indicates no matrix effect, signal enhancement and signal suppression, respectively.

The recovery of Rh6G added at 3 different concentrations (10^{-9}, 10^{-7} and 10^{-5} M) separately to food samples, followed by QuEChERS extraction and analysis by GE-AuNPs/GO SERS method showed a recovery and RSD values ranging from 91.0–95.4% and 2.4–8.3% for red chilli pepper powder, 96.6–98.3% and 6.3–9.0% for red glutinous rice ball and 98.9–102.3% and 3.8–8.4% for tomato ketchup, respectively (Table 2). Fig. 5B–E shows the representative SERS spectra obtained by using GE-AuNPs/GO for detection of Rh6G spiked at 1×10^{-9} M separately into tap water, red chilli pepper powder, red glutinous rice ball and tomato ketchup. These high recovery values with RSD <9% implied that the developed GE-AuNPs/GO SERS method can be successfully applied to food samples. In addition, the Rh6G recovery from these food samples followed the order: tomato ketchup > red glutinous rice ball > red chilli pepper powder which correlated well with their slope ratios (1.03, 0.98 and 0.95) of the matrix effects as shown above. Wang et al. (2020b) also reported a similar recovery value ranging from 94.0–106.2% and RSD from 1.7–4.6% for three spiked Rh6G levels (10^{-10}, 10^{-9} and 10^{-8} M) in orange juice. However, a relatively higher RSD value obtained in our study may be due to a more complicated matrix in solid food samples used in our study.

4. Conclusions

A simple, fast and cost-effective paper-based SERS method was developed by using grape skin waste extract-capped gold nanoparticles anchored on graphene oxide for onsite detection of rhodamine 6G in water and food. Compared to normal Raman spectra, an enhancement factor as high as 1.92×10^{9} was shown for rhodamine 6G signals, accompanied by a low detection limit at 7.33×10^{-11} M in the linear range of 10^{-11}–10^{-5} M. A high repeatability within a SERS substrate and high reproducibility between different SERS substrates revealed that the developed paper-based GE-AuNPs/GO SERS method can be successfully applied for sensitive detection of organic toxins like rhodamine 6G. Also, a high stability with only a minimum loss in SERS efficiency was observed during 60-day storage of GE-AuNPs/GO substrate. Application to tap water and food samples showed a high recovery of rhodamine 6G, demonstrating that the paper-based GE-AuNPs/GO substrate can be a promising alternative for SERS detection of organic toxins especially rhodamine 6G in water and food.

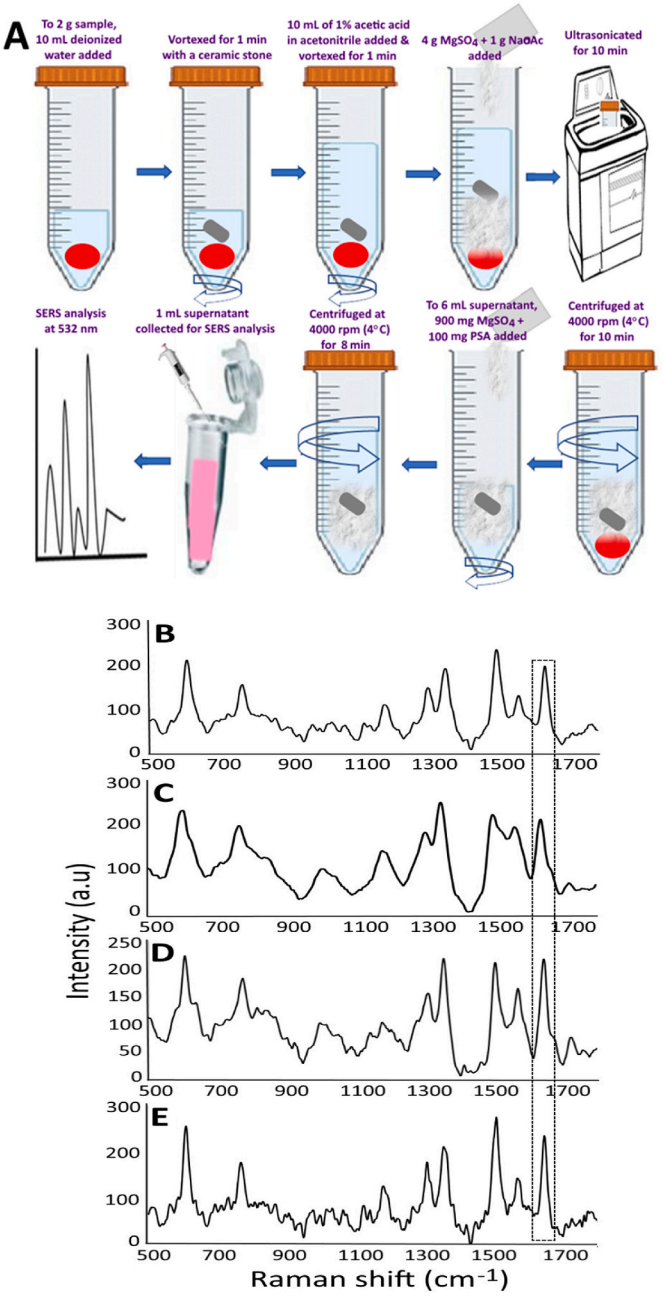

Fig. 5. The sequential steps involved in extraction of Rh6G from food samples by QuEChERS method (A) and SERS spectra for detection of Rh6G (1×10^{-9} M) spiked separately into tap water (B), red chilli pepper powder (C), red glutinous rice ball (D) and tomato ketchup (E) by using GE-AuNPs/GO substrate. For detection of Rh6G from 3 food samples, Rh6G was initially extracted and purified by QuEChERS method prior to detection by the GE-AuNPs/GO SERS method. Rh6G, rhodamine 6G; QuEChERS, quick, easy, cheap, effective, rugged and safe; SERS, surface enhanced Raman scattering; $MgSO_4$, magnesium sulfate; NaOAc, sodium acetate; PSA, primary secondary amine; GE-AuNPs/GO, grape skin extract-stabilized gold nanoparticles anchored on graphene oxide; a. u, arbitrary unit. (For interpretation of the references to color in this figure legend, the reader is referred to the Web version of this article.)

Credit author statement

Kandi Sridhar: Methodology, Investigation, Validation, Date curation, Formal analysis, Software, Data curation, Visualization, Writing – original draft; **Baskaran Stephen Inbaraj**: Conceptualization, Methodology, Investigation, Validation, Formal analysis, Data curation, Visualization, Writing – original draft, Writing – review & editing; **Bing-Huei Chen**, Conceptualization, Methodology, Resources, Supervision, Project administration, Validation, Writing – review & editing.

Declaration of competing interest

The authors declare that they have no known competing financial interests or personal relationships that could have appeared to influence the work reported in this paper.

Acknowledgements

This study was supported by a grant from the Ministry of Science and Technology, Taiwan (MOST 109-2221-E-030-005). The authors wish to thank Mr. Yen-Sheng Wu from Tzong Jao Hang's Electron Microscope Laboratory, School of Medicine, Fu Jen Catholic University, Taipei, Taiwan, for technical assistance in recording TEM images.

Appendix A. Supplementary data

Supplementary data to this article can be found online at https://doi.org/10.1016/j.chemosphere.2022.134702.

References

Adam, M., Bajer, T., Bajerová, P., Ventura, K., 2018. Modified QuEChERS approach for analysis of synthetic food dyes in jellies and smarties. Food Anal. Met. 11, 1619–1626.

Bai, S., Serien, D., Hu, A., Sugioka, K., 2018. 3D Microfluidic surface-enhanced Raman spectroscopy (SERS) chips fabricated by all-femtosecond-laser-processing for real-time sensing of toxic substances. Adv. Funct. Mat. 28, 1706262.

Baron, G., Ferrario, G., Marinello, C., Carini, M., Morazzoni, P., Aldini, G., 2021. Effect of extraction solvent and temperature on polyphenol profiles, antioxidant and anti-inflammatory effects of red grape skin by-product. Molecules 26, 5454.

Baskoro, F., Wong, C.-B., Kumar, S.R., Chang, C.-W., Chen, C.-H., Chen, D.W., Lue, S.J., 2018. Graphene oxide-cation interaction: Inter-layer spacing and zeta potential changes in response to various salt solutions. J. Mem. Sci. 554, 253–263.

Brady, E., Burgess, J., 2015. Determination of Triphenylmethane Dyes and Their Metabolites in Shrimp Using QuEChERS Extraction and the ACQUITY UPLC H-Class System with Xevo TQD. Waters Corporation, Milford, MA, USA. Retrieved from. https://www.waters.com/webassets/cms/library/docs/720005307en.pdf.

Can, M., 2020. Green gold nanoparticles from plant-derived materials: an overview of the reaction synthesis types, conditions, and applications. Rev. Chem. Engg. 36, 859–877.

Castillo-Henríquez, L., Alfaro-Aguilar, K., Ugalde-Álvarez, J., Vega-Fernández, L., Montes de Oca-Vásquez, G., Vega-Baudrit, J.R., 2020. Green synthesis of gold and silver nanoparticles from plant extracts and their possible applications as antimicrobial agents in the agricultural area. Nanomaterials 10, 1763.

Chiang, C.-Y., Liu, T.-Y., Su, Y.-A., Wu, C.-H., Cheng, Y.-W., Cheng, H.-W., Jeng, R.-J., 2017. Au nanoparticles immobilized on honeycomb-like polymeric films for surface-enhanced Raman scattering (SERS) detection. Polymers 9, 93.

Dalla Marta, S., Novara, C., Giorgis, F., Bonifacio, A., Sergo, V., 2017. Optimization and characterization of paper-made surface enhanced Raman scattering (SERS) substrates with Au and Ag NPs for quantitative analysis. Materials 10, 1365.

Dash, S.S., Bag, B.G., Hota, P., 2014. *Lantana camara* Linn leaf extract mediated green synthesis of gold nanoparticles and study of its catalytic activity. App. Nanosci. 5, 343–350.

Elia, P., Zach, R., Hazan, S., Kolusheva, S., Porat, Z., Zeiri, Y., 2014. Green synthesis of gold nanoparticles using plant extracts as reducing agents. Int. J. Nanomed. 9, 4007–4021.

EU, 2011. The Annexure to Regulation (EC) No. 1881/2006) of August 20, 2011, Section 6: Maximum Allowable Levels of Benzo[a]pyrene and 4 Polycyclic Aromatic Hydrocarbons Combined. Official J. Eur. Union. L215, 1-7. Retrieved from. https://eur-lex.europa.eu.

González-Ballesteros, N., Rodríguez-González, J.B., Rodríguez-Argüelles, M.C., 2018. Harnessing the wine dregs: an approach towards a more sustainable synthesis of gold and silver nanoparticles. J. Photochem. Photobio. B: Bio. 178, 302–309.

Hamzah, F.G., Humud, H.R., 2021. Highly sensitive detection of Raman scattering to Rhodamine 6G dyes based on SERS for roughened plasmonic nanostructures. AIP Conf. Proc. 2372, 080021.

Hua, L.-H., Inbaraj, B.S., Chen, B.H., 2021. An improved analytical method for determination of trans-resveratrol and related stilbenes in grape skin by QuEChERS coupled with HPLC-PDA-MS. Int. J. Food Sci. Technol. 56, 6376–6387.

Huang, J., Zhang, L., Chen, B., Ji, N., Chen, F., Zhang, Y., Zhang, Z., 2010. Nanocomposites of size-controlled gold nanoparticles and graphene oxide: formation and applications in SERS and catalysis. Nanoscale 2, 2733–2738.

Hung, Y.-T., Lee, Y.-T., Inbaraj, B.S., Sridhar, K., Chen, B.-H., 2021. Analysis and formation of polycyclic aromatic hydrocarbons and cholesterol oxidation products in thin slices of dried pork during processing. Food Chem. 353, 129474.

Inbaraj, B.S., Chen, B.Y., Liao, C.W., Chen, B.H., 2020. Green synthesis, characterization and evaluation of catalytic and antibacterial activities of chitosan, glycol chitosan and poly(γ-glutamic acid) capped gold nanoparticles. Int. J. Biol. Macromol. 161, 1484–1495.

Inbaraj, B.S., Sridhar, K., Chen, B.-H., 2021a. Removal of polycyclic aromatic hydrocarbons from water by magnetic activated carbon nanocomposite from green tea waste. J. Hazar. Mat. 415, 125701.

Inbaraj, B.S., Hua, L.H., Chen, B.H., 2021b. Comparative study on inhibition of pancreatic cancer cells by resveratrol gold nanoparticles and a resveratrol nanoemulsion prepared from grape skin. Pharmaceutics 13, 1871.

Kavitha, C.N., Bramhaiah, K., John, N.S., Ramachandran, B.E., 2015. Low cost, ultra-thin films of reduced graphene oxide-Ag nanoparticle hybrids as SERS based excellent dye sensors. Chem.Phy. Lett. 629, 81–86.

Krishnaswamy, K., Vali, H., Orsat, V., 2014. Value-adding to grape waste: green synthesis of gold nanoparticles. J. Food Engg. 142, 210–220.

Langer, J., Jimenez de Aberasturi, D., Aizpurua, J., Alvarez-Puebla, R.A., Auguié, B., Baumberg, J.J., Bazan, G.C., Bell, S.E.J., Boisen, A., Brolo, A.G., Choo, J., Cialla-May, D., Deckert, V., Fabris, L., Faulds, K., García de Abajo, F.J., Goodacre, R., Graham, D., Haes, A.J., Haynes, C.L., Huck, C., Itoh, T., Käll, M., Kneipp, J., Kotov, N.A., Kuang, H., Le Ru, E.C., Lee, H.K., Li, J.-F., Ling, X.Y., Maier, S.A., Mayerhöfer, T., Moskovits, M., Murakoshi, K., Nam, J.-M., Nie, S., Ozaki, Y., Pastoriza-Santos, I., Perez-Juste, J., Popp, J., Pucci, A., Reich, S., Ren, B., Schatz, G. C., Shegai, T., Schlücker, S., Tay, L.-L., Thomas, K.G., Tian, Z.-Q., Van Duyne, R.P., Vo-Dinh, T., Wang, Y., Willets, K.A., Xu, C., Xu, H., Xu, Y., Yamamoto, Y.S., Zhao, B., Liz-Marzán, L.M., 2020. Present and future of surface-enhanced Raman scattering. ACS Nano 14, 28–117.

Lee, D.-J., Kim, D.Y., 2019. Hydrophobic paper-based SERS sensor using gold nanoparticles arranged on graphene oxide flakes. Sensors 19, 5471.

Lee, H.K., Lee, Y.H., Koh, C.S.L., Phan-Quang, G.C., Han, X., Lay, C.L., Sim, H.Y.F., Kao, Y.-C., An, Q., Ling, X.Y., 2019. Designing surface-enhanced Raman scattering (SERS) platforms beyond hotspot engineering: emerging opportunities in analyte manipulations and hybrid materials. Chem. Soc. Rev. 48, 731–756.

Lee, K.X., Shameli, K., Miyake, M., Khairudin, N.B.B.A., Mohamad, S.E.B., Hara, H., Nordin, M.F.B.M., Yew, Y.P., 2017. Gold nanoparticles biosynthesis: a simple route for control size using waste peel extract. IEEE Transac. Nanotechnol. 16, 954–957.

Lee, K.X., Shameli, K., Yew, Y.P., Teow, S.Y., Jahangirian, H., Rafiee-Moghaddam, R., Webster, T.J., 2020. Recent Developments in the facile bio-synthesis of gold nanoparticles (AuNPs) and their biomedical applications. Int. J. Nanomed. 15, 275–300.

Lee, M., Oh, K., Choi, H.-K., Lee, S.G., Youn, H.J., Lee, H.L., Jeong, D.H., 2018. Subnanomolar sensitivity of filter paper-based SERS sensor for pesticide detection by hydrophobicity change of paper surface. ACS Sens. 3, 151–159.

Li, J.-F., Zhang, Y.-J., Ding, S.-Y., Panneerselvam, R., Tian, Z.-Q., 2017. Core–shell nanoparticle-enhanced Raman spectroscopy. Chem. Rev. 117, 5002–5069.

Nan, H., Chen, Z., Jiang, J., Li, J., Zhao, W., Ni, Z., Gu, X., Xiao, S., 2018. The effect of graphene on surface plasmon resonance of metal nanoparticles. Phy. Chem. Chem. Phy. 20, 25078–25084.

Nancy, P., Nair, A.K., Antoine, R., Thomas, S., Kalarikkal, N., 2019. *In situ* decoration of gold nanoparticles on graphene oxide via nanosecond laser ablation for remarkable chemical sensing and catalysis. Nanomaterials 9, 1201.

Oh, K., Lee, M., Lee, S.G., Jung, D.H., Lee, H.L., 2018. Cellulose nanofibrils coated paper substrate to detect trace molecules using surface-enhanced Raman scattering. Cellulose 25, 3339–3350.

Ouhibi, A., Saadaoui, M., Lorrain, N., Guendouz, M., Raouafi, N., Moadhen, A., 2020. Application of doehlert matrix for an optimized preparation of a surface-enhanced Raman spectroscopy (SERS) substrate based on silicon nanowires for ultrasensitive detection of rhodamine 6G. Appl. Spectrosc. 74, 168–177.

Pino, E., Calderón, C., Herrera, F., Cifuentes, G., Arteaga, G., 2020. Photocatalytic degradation of aqueous rhodamine 6G using supported TiO_2 catalysts. A model for the removal of organic contaminants from aqueous samples. Front. Chem. 8, 365.

Punniyakotti, P., Aruliah, R., Angaiah, S., 2021. Facile synthesis of reduced graphene oxide using *Acalypha indica* and *Raphanus sativus* extracts and their *in vitro* cytotoxicity activity against human breast (MCF-7) and lung (A549) cancer cell lines. 3 Biotech 11, 157.

Rajoriya, S., Bargole, S., Saharan, V.K., 2017. Degradation of a cationic dye (Rhodamine 6G) using hydrodynamic cavitation coupled with other oxidative agents: reaction mechanism and pathway. Ultrasonic. Sonochem. 34, 183–194.

Shahriari, S., Sastry, M., Panjikar, S., Singh Raman, R.K., 2021. Graphene and graphene oxide as a support for biomolecules in the development of biosensors. Nanotechnol. Sci. Appli. 14, 197–220.

Shi, G.C., Wang, M.L., Zhu, Y.Y., Shen, L., Ma, W.L., Wang, Y.H., Li, R.F., 2018. Dragonfly wing decorated by gold nanoislands as flexible and stable substrates for surface-enhanced Raman scattering (SERS). Sci. Rep. 8, 6916.

Singh, J., Mehta, A., 2020. Rapid and sensitive detection of mycotoxins by advanced and emerging analytical methods: a review. Food Sci. Nutri. 8, 2183–2204.

Wang, J., Qiu, C., Mu, X., Pang, H., Chen, X., Liu, D., 2020a. Ultrasensitive SERS detection of rhodamine 6G and p-nitrophenol based on electrochemically roughened nano-Au film. Talanta 210, 120631.

Wang, J., Li, J., Zeng, C., Qu, Q., Wang, M., Qi, W., Su, R., He, Z., 2020b. Sandwich-like sensor for the highly specific and reproducible detection of Rhodamine 6G on a surface-enhanced Raman scattering platform. ACS Appl. Mater. Interfaces 12, 4699–4706.

Xiao, N., Deng, J., Huang, K., Ju, S., Hu, C., Liang, J., 2014. Application of derivative and derivative ratio spectrophotometry to simultaneous trace determination of rhodamine B and rhodamine 6G after dispersive liquid-liquid microextraction. Spectrochim. Acta Part A: Mol. Biomol. Spectro. 128, 312–318.

Yeh, Y.-C., Creran, B., Rotello, V.M., 2012. Gold nanoparticles: preparation, properties, and applications in bionanotechnology. Nanoscale 4, 1871–1880.

Yu, J., Ma, Y., Yang, C., Zhang, H., Liu, L., Su, J., Gao, Y., 2018. SERS-active composite based on rGO and Au/Ag core-shell nanorods for analytical applications. Sens. Actuat. B: Chem. 254, 182–188.

Zhang, C.-Y., Hao, R., Zhao, B., Hao, Y.-W., Liu, Y.-Q., 2017. A ternary functional Ag@GO@Au sandwiched hybrid as an ultrasensitive and stable surface enhanced Raman scattering platform. Appl.Surf. Sci. 409, 306–313.

Zhao, Y., Li, X., Du, Y., Chen, G., Qu, Y., Jiang, J., Zhu, Y., 2014. Strong light–matter interactions in sub-nanometer gaps defined by monolayer graphene: toward highly sensitive SERS substrates. Nanoscale 6, 11112–11120.

Zhou, H., Li, X., Wang, L., Liang, Y., Jialading, A., Wang, Z., Zhang, J., 2021. Application of SERS quantitative analysis method in food safety detection. Rev. Anal. Chem. 40, 173–186.